



Universiteit  
Leiden  
The Netherlands

## Mining the kinematics of discs to hunt for planets in formation

Izquierdo Cartagena, A.F.

### Citation

Izquierdo Cartagena, A. F. (2023, December 1). *Mining the kinematics of discs to hunt for planets in formation*. Retrieved from <https://hdl.handle.net/1887/3665447>

Version: Publisher's Version

License: [Licence agreement concerning inclusion of doctoral thesis in the Institutional Repository of the University of Leiden](#)

Downloaded from: <https://hdl.handle.net/1887/3665447>

**Note:** To cite this publication please use the final published version (if applicable).

# Chapter 1

---

## Introduction

---

Our ancestors used to gaze at the night sky in search for answers to the meaning of our existence, and we are not exempt from this tradition. Although our place in the universe remains an open philosophical question, modern and contemporary astronomical research has propelled us closer to attempting to address the “how” of our origin. In less than five centuries, we have progressed from adopting a heliocentric model for our solar system to photograph the event horizon of black holes. Just a little over a century ago, we had no inkling of the existence of galaxies beyond our own, and today we possess the tools to estimate that there should be hundreds of billions of galaxies out there in the observable universe. Scaling back to less extreme levels, in a mere matter of decades, we have transitioned from being aware of only eight planets in our immediate vicinity to spotting thousands of extrasolar planets orbiting stars in our Galactic neighbourhood. Aided by cutting-edge telescopes, spectrographs, and computational capabilities, we can now not only identify these exoplanets but also deduce their mass and orbital characteristics, and even study the chemical makeup of their atmospheres. By examining the places where planets originate, protoplanetary discs, we are beginning to trace the key ingredients that contribute to their eventual composition and attributes as fully developed objects, bringing us significantly closer to comprehending our own origins. After all, it appears that our predecessors were indeed looking in the right direction.

This thesis centres on a particular aspect of the planet formation history. It presents and employs a novel methodology for the detection of signatures driven by giant planets still embedded in gas-rich discs orbiting young Solar-type stars. The emergence of giant planets in discs is a pivotal facet of the assembly history of planetary systems as it can greatly influence the evolution and transport of gaseous and dusty matter—essential building blocks for nascent planets—throughout much of the disc radial and vertical extent. Before delving into the specifics of young planet detection, I will outline the primary aspects of our current understanding on the formation of stars, discs, and planets. Additionally, I will briefly touch

upon our knowledge of the physical and dynamical structure characterising the discs that serve as the cradle for planet formation.

## 1.1 Young Stellar Objects

The formation of stars is a natural consequence of the evolution of matter in galaxies. The cold ( $\sim 1 - 30\text{K}$ ) and dense ( $\sim 10^3 - 10^7\text{cm}^{-3}$ ) portion of this matter where stellar birth occurs is embodied in the form of giant molecular clouds, primarily composed of molecular hydrogen ( $\text{H}_2$ ), along with some atomic hydrogen, helium, and dust grains. More complex and heavier molecules mainly consisting of carbon, oxygen, hydrogen, and nitrogen atoms, can also assemble within these regions. CO, for example, the most prevalent molecule after  $\text{H}_2$ , forms through the interplay between photodissociation and photoionization reactions, regulated by far-ultraviolet photons, and attenuation mechanisms such as dust absorption and scattering,  $\text{H}_2$  shielding, and self-shielding (van Dishoeck & Black 1988; Hollenbach & Tielens 1999).

In our present-day Galaxy, the process of star formation begins with the emergence of density fluctuations within these clouds, triggered by the intricate interaction between (both galactic and local) gravitational forces and magneto-hydrodynamical turbulence fueled by supernova explosions and stellar feedback mechanisms (see e.g. Gatto et al. 2015; Federrath 2018; Smith et al. 2020; Izquierdo et al. 2021a). Over time, regions of high density driven by these factors undergo gravitational instabilities, leading to the formation of clumps. These clumps subsequently collapse into smaller gravitationally bound cores, marking the embryonic phase of what will potentially evolve, over millions of years, into a main sequence star and a planetary system. Let us now briefly walk through the evolutionary journey of these young stellar objects.

### 1.1.1 Low-mass star formation

If the mass of the protostellar core falls within the lower range ( $M < 8 M_\odot$ ), the progression of the nascent system tends to unfold in a series of relatively well-defined stages as depicted in Figure 1.1. Astronomers have established empirical classification criteria for such systems, rooted in observables derived from the distribution of dust surrounding the protostar. This distribution seems to be connected to the age of the emerging system and is discerned by examining the shape of the spectral energy distribution of the dust emission at near- and mid-infrared wavelengths (Adams et al. 1987; Lada 1987).

Class 0 objects epitomize the earliest observable stage of stellar evolution and can persist for as brief a duration as  $10^5\text{yr}$  (Dunham et al. 2014). These sources are characterised by their hosting of massive and dense envelope structures of gas and dust ( $M_{\text{env}} > M_\star$ ), and are virtually imperceptible at mid- and near-infrared wavelengths due to the obscuring presence of surrounding material. Consequently, this category was not included in the original classification system proposed by Adams et al. (1987), but it was added shortly afterward due to compelling evidence

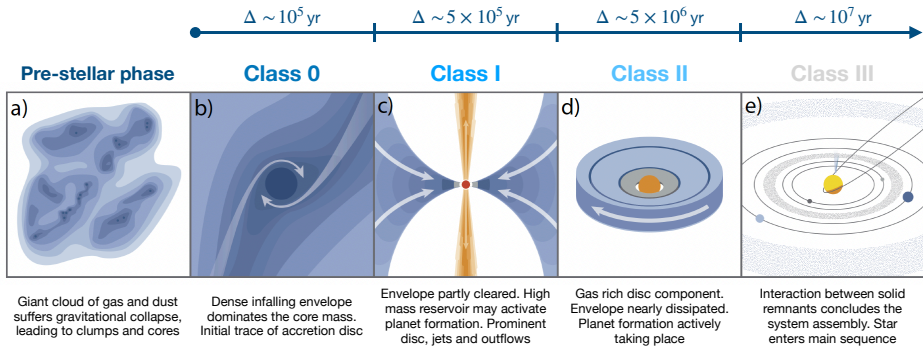


**Figure 1.1:** Schematic view of the evolution of low-mass Young Stellar Objects (YSOs) (adapted from Öberg & Bergin 2021).

suggesting the presence of cores with molecular outflows observed at sub-millimeter wavelengths (André et al. 1993; Barsony 1994). During this stage, a significant amount of infalling material is accreted onto the protostar at a rate of  $\dot{M} > 10^{-6} M_{\odot} \text{ yr}^{-1}$ , while another portion initiates the formation of an accretion disc around the nascent star. This phenomenon arises from the necessity to conserve angular momentum: As material spirals inward toward the centre of the system, its orbital velocity increases, leading to stronger and stabilising centripetal forces in the plane perpendicular to the axis of angular momentum. Consequently, a portion of the collapsing core gradually flattens, thus marking the emergence of the disc component.

Class I sources are identified subsequent to the partial dissipation of the circumstellar envelope. In this phase, a flattened disc component emerges from the embedded state, giving rise to significant infrared radiation in addition to the black-body emission from the protostar. This phase can persist for approximately  $\sim 5 \times 10^5$  yr (Dunham et al. 2014). Despite a considerable portion of the envelope having been either accreted or dispersed in the previous stage due to internal and external stellar feedback, it still plays a significant role during this phase, continually transferring substantial amounts of mass and angular momentum into the disc component. As the disc accumulates mass, gravitational instabilities are susceptible to occurring, prompting the formation of agglomerations and spiral density waves (Kratte & Lodato 2016). These phenomena facilitate the transport of angular momentum and contribute to maintaining high mass accretion rates of around  $\dot{M} \approx 10^{-6} M_{\odot} \text{ yr}^{-1}$  onto the star. Such elevated accretion rates, however, lead the system to expel some of the excess angular momentum in the form of outflows and jets. It is also worth highlighting that, owing to the substantial reservoir of mass present at this stage, it has been postulated that planetary assembly might need to commence this early to account for the observed amount and distribution of high-mass planets in fully-formed systems (see e.g. Tychoniec et al. 2020, and references therein).

Class II objects, the concluding and most enduring gas-rich phase spanning

several  $10^6$  yr, embody a stage where the envelope is largely absent. The majority of this component has either been accreted, initially onto the disc and subsequently onto the star, or expelled from the system in the form of outflows, rendering these sources excellent candidates for direct analyses of the initial stages of planet formation at infrared and millimeter wavelengths. Although the remaining circumstellar disc accounts for a modest fraction of the total mass of the system ( $<10\%$  of the stellar mass, Kama et al. 2020), it still wields enough influence to induce an infrared excess on the observed spectral energy distribution. By this point, the protostar has already accreted the majority of its mass and has embarked on a pre-main sequence evolutionary track, where it gradually contracts until reaching (quasi-)hydrostatic equilibrium, becoming a mature main-sequence star (Hayashi 1961, 1966). It is also at this stage where the bulk of the assembly of the planetary system occurs, their solid content is glued, their orbital parameters and mass are set, and the chemical composition of their atmospheres is ultimately determined. This thesis is dedicated to the study of the kinematic signatures and gas substructures driven by planets embedded in systems falling into this category.

Finally, Class III sources, primarily consist of a disc of solid remnants from the process of star and planet formation. In this phase, the emission is largely dominated by the black-body stellar radiation, and the mass accretion rate onto the star ceases. As the disc material is used up or dispersed for the next  $\sim 10^7$  yr, the star is considered to have fully reached the end of its formation path.

## 1.1.2 Physical and dynamical structure of discs

Once the envelope has been substantially cleared, the disc component becomes the dominant circumstellar structure of the nascent system for several million years. During this period, planets have ample time to finalise their assembly through accretion and coagulation mechanisms, and thus, this component is referred to as a protoplanetary disc. The interplay between the balance of forces and the transport of angular momentum to sustain the culminating accretion phase onto the star shapes the structure and dynamics of these objects.

### 1.1.2.1 Density and temperature structure

In good approximation, assuming for now that the stellar gravity dominates over the disc self-gravity contribution along the vertical direction, hydrostatic equilibrium requires,

$$\frac{1}{\rho} \frac{\partial P}{\partial z} = - \frac{GM_{\star}}{(R^2 + z^2)^{3/2}} z, \quad (1.1)$$

where  $P$  is pressure and  $\rho$  is the gas volume density,  $G$  is the gravitational constant,  $R$  denotes the cylindrical radial coordinate relative to the centre of the system, and  $z$  is the vertical displacement of the fluid element from the disc midplane. Adopting an ideal gas equation of state,  $P = \rho c_s^2$ , where  $c_s \propto T^{1/2}$  represents the isothermal sound speed, and considering that the temperature distribution solely depends on the radial coordinate, this differential equation can be trivially solved

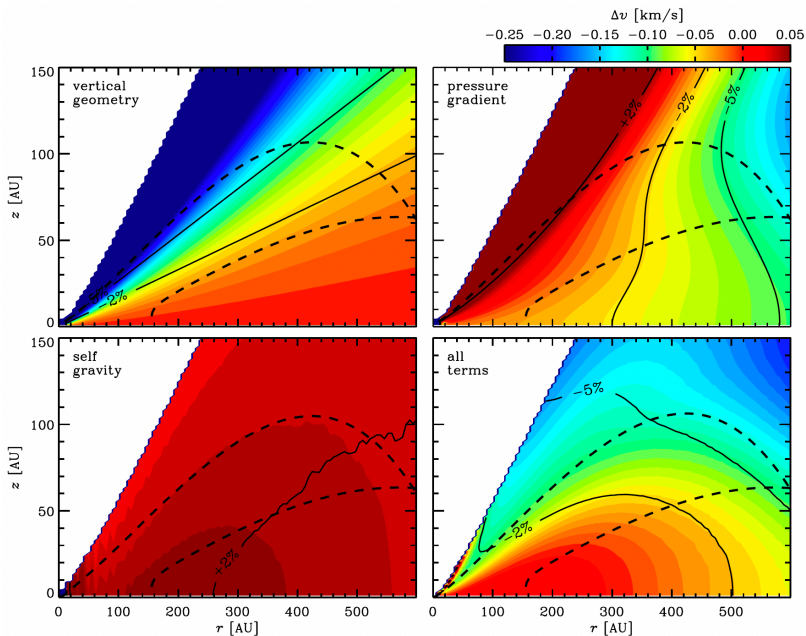


**Figure 1.2:** Magnitude of deviations from Keplerian motion in a model disc subject to different gravitational and pressure forces. Solid contours highlight percentage deviations from Keplerian, and the dashed lines indicate the region of the disc where CO is in gas phase, and thus accessible with ALMA through CO isotopologue emission as discussed in Sect. 1.2.2. Credits: Rosenfeld et al. (2013).

for the gas volume density,

$$\rho(R, z) = \rho_0(R) \exp \left[ -\frac{R^2}{H^2} \left( 1 - \frac{1}{\sqrt{1 + z^2/R^2}} \right) \right], \quad (1.2)$$

where  $H(R) = c_s/\Omega_K$  is the pressure scale height at the midplane, and  $\Omega_k = (GM_*/R^3)^{1/2}$  is the Keplerian angular velocity.

According to the theory of viscous accretion, the transport of angular momentum is instigated by turbulent motions in the disc gas (Lynden-Bell & Pringle 1974a; Pringle 1981; Hartmann et al. 1998). The origin of this turbulence is still subject of debate, but a strong candidate mechanism is the magneto-rotational instability (MRI), triggered by the influence of weak magnetic fields on ionized fluid in the upper layers of the disc, as well as other purely hydrodynamical processes (see Lesur et al. 2023; Rosotti 2023, for theoretical and observational reviews, respectively). The effect of viscosity causes material in the inner disc to transfer angular momentum to the outer disc, inducing an inward motion of the former while the outer component shifts away from the star. The magnitude of these turbulent motions is quantified by an alpha-viscosity parameter, which is assumed to be constant at first order but can potentially vary with the radial location and

depth along the disc vertical direction.

Although viscous accretion also functions as a heat source by dissipating rotational energy, stellar irradiation takes precedence as the primary heat source in protoplanetary discs. This radiation is absorbed and redistributed by dust grains, with an intensity and direction determined by the grain surface geometry and composition. The way the disc vertical extent varies with radius is also an important factor of the heating process as it establishes how incident radiation penetrates and propagates through the inner layers of the disc (Turner et al. 2012). Radiative transfer models that take these ingredients into account conclude that the temperature distribution of flared irradiated discs around T Tauri stars should vary differently with radius in the upper layers compared to layers closer to the midplane (see e.g. Dartois et al. 2003).

However, it is important to note that gas and dust temperatures are not inherently coupled. In certain regions of the disc, gas-dust collisions are infrequent and therefore less influential than other cooling mechanisms, such as line radiation, when it comes to determining the gas temperature. This disparity becomes more pronounced in low-density areas, like cavities or gaps, which numerous observations suggest are common features in discs or, at the very least, prevalent among relatively large discs that can be resolved with current instrumentation (see Section 1.2.2). Using thermo-chemical models that self-consistently account for the balance between heating and cooling mechanisms becomes imperative for detailed studies of the temperature structure in these more complex scenarios (see e.g. Bruderer et al. 2012; Bruderer 2013; Woitke et al. 2016).

### 1.1.2.2 Dynamical structure

To calculate the magnitude of the disc rotational velocity around its parent star we must analyse the presence of central forces at play in the system. These forces are usually dominated by internal gravitational fields and pressure gradients. Assuming a slowly accreting disc, the balance of central forces requires,

$$v_{\phi}^2(R, z) = R \frac{\partial \Phi}{\partial R} + \frac{R}{\rho} \frac{\partial P}{\partial R}, \quad (1.3)$$

where  $\Phi$  stands for the gravitational potential acting in the disc, and encloses not only the contribution from the star, but also that of the disc itself.

At first order, the disc rotational velocity can be assumed to be Keplerian as the stellar gravity is expected to carry most of the central force magnitude in this evolutionary phase of the system, meaning that the velocity would be solely determined by the stellar mass and orbital radius of the fluid element analysed,

$$v_{\phi}(R) = v_K \equiv \sqrt{\frac{GM_{\star}}{R}}. \quad (1.4)$$

Nevertheless, discs in this phase usually have sufficient temperature and gas mass to be geometrically thick, to a degree that molecular line observations have been able to systematically resolve for over a decade (see e.g. de Gregorio-Monsalvo

et al. 2013; Rosenfeld et al. 2013; Pinte et al. 2018a; Law et al. 2021b; Paneque-Carreño et al. 2023). Therefore, a better approximation involves considering the vertical coordinate too,

$$v_\phi(R, z) = \sqrt{\frac{GM_\star}{(R^2 + z^2)^{3/2}}} R, \quad (1.5)$$

which implies differential rotation as a function of height, with a magnitude decreasing as one moves up (or down) relative to the disc midplane. This expression is the result of hydrostatic equilibrium along the disc vertical direction, where the vertical component of the gravitational force from the star cancels out the opposing pressure force (i.e. Eq. 1.1), leaving only the component of the stellar gravity parallel to the disc midplane operate as the central force.

Naturally, pressure forces not only act vertically but also radially, thereby also playing a role in shaping the rotational velocity of protoplanetary discs. The radial pressure force typically performs from the inside out, because it points in the opposite direction of increasing temperature and density gradients. Plugging Eqs. 1.1 and 5.1 into Eq. 1.3; using  $P = \rho c_s^2$  again; assuming that the density normalisation follows  $\rho_0(R) \propto R^{-q_d}$ , and that the temperature is vertically isothermal  $T(R) \propto R^{-q_t}$ , it is possible to write an analytical expression for  $v_\phi$  in terms of both the contribution of stellar gravity and pressure parameters (Lodato et al. 2022),

$$v_\phi = \sqrt{\frac{GM_\star}{R}} \left[ 1 - q_p \left( \frac{H}{R} \right)^2 - q_t \left( 1 - \frac{R}{\sqrt{R^2 + z^2}} \right) \right]^{1/2}, \quad (1.6)$$

where  $q_p = 3/2 + q_d + q_t$  is the power-law exponent of the pressure radial profile. Note that the expression in brackets is always smaller than one, and that the multiplying factor is simply the Keplerian velocity,  $v_K$  (Eq. 1.4). In practice, this means that under the aforementioned assumptions, a decreasing pressure gradient induces material to rotate at a sub-Keplerian pace around the star, and that such an effect becomes more noticeable at large radii where the disc is thicker.

Finally, the radial component of the disc gravitational field can also play a role if the disc mass reservoir is high. Under similar assumptions on the temperature and density structure it is possible to calculate this contribution in terms of the disc cylindrical coordinates solving a semi-analytical expression that depends on the surface density distribution (see e.g. Bertin & Lodato 1999).

However, if no assumptions are made on the underlying temperature structure, the combined impact of this and the latter two forces on the disc velocity field must be calculated iteratively through the use of numerical methods, as in Rosenfeld et al. (2013), for example. Figure 1.2 illustrates the differences in considering the various contributions to the rotational velocity compared to the purely Keplerian component, obtained by only assuming hydrostatic equilibrium and centrifugal balance. Depending on the location of the fluid element, one or the other component may dominate. In higher layers, the differential rotation generated by vertical hydrostatic balance prevails, showing deviations from Keplerian rotation larger than 5% at scale heights of  $z/r \approx 0.3$ , where CO, the most abundant and



commonly used tracer for kinematical studies of discs, typically emits (see e.g. Law et al. 2021b; Paneque-Carreño et al. 2023). Driven by pressure forces, a similar order of deviations is observed in the outer regions of the disc, but with the opposite sign due to the negative radial gradient of temperature and density. Last, the disc self-gravity component can dominate in regions near the midplane. The relevance of this latter component is, of course, subject to the available amount of disc mass. Recent high velocity resolution observations suggest that the percentage deviations from pure Keplerian rotation due to this force can be as large as 10% in massive targets ( $M_d \approx 0.1M_\star$ ) even in the disc upper layers (see e.g. Veronesi et al. 2021; Lodato et al. 2022).

### 1.1.3 Disc observations

The collective endeavours of ground-based telescopes, space missions, and cutting-edge interferometers have fundamentally transformed our understanding of protostellar and protoplanetary discs. These facilities have not merely validated the presence of such circumstellar structures but also exposed their intricate complexity and their vital role in the formation of planets. Let's briefly explore the key historical aspects and instruments that have contributed to shaping the current understanding of this field.

#### 1.1.3.1 Historical remarks

During the late 1970s and early 1980s, pioneering ground- and space-based observatories provided the initial evidence suggesting that young pre-main sequence stars retain circumstellar material even after their original infalling envelope has dissipated. Some of the evidence included strong linear polarization in optical and infrared wavelengths, indicative of starlight scattered by dust grains and electrons distributed in non-spherical shells around the protostar (see Elsasser & Staude 1978, and references therein), significant excess emission in the infrared (Cohen 1983; Grasdalen et al. 1984), and the presence of large-scale structures, such as optical jets and bipolar molecular outflows generally aligned with the magnetic field direction (Snell et al. 1980; Bastien 1982; Hodapp 1984). These phenomena were interpreted in terms of a flattened disc-like distribution of matter around the protostar (see Beckwith & Sargent 1993b, for a review) and served as the motivation for subsequent systematic studies of spectral energy distributions around nearby star-forming regions in the years that followed (see e.g. Rucinski 1985). Ultimately, these studies led to the development of a classification system that describes the evolutionary phases of Young Stellar Objects (YSOs) (Adams et al. 1987; Lada 1987), as summarised in Section 1.1, and which is widely accepted in contemporary times.

The first direct evidence of a rotating circumstellar disc, however, emerged with the advent of millimeter-wave interferometers, which enabled the resolved imaging of both thermal radiation from cold dust and line emission from dense molecular species. Utilising the Owens Valley Radio Observatory (OVRO), Sargent & Beckwith (1987) identified a flattened structure around the T-Tauri star

HL Tau in  $^{13}\text{CO}$  emission, and demonstrated that the gas velocity traced by this molecule followed Keplerian motion, a characteristic of disc rotation dominated by the gravitational potential of the central star, as discussed in Section 1.1.2. Just a few years later, infrared ground- and space-based photometry targeting the same type of stars noticed that a subset of them exhibited near- and mid-infrared deficits, in contrast to the standard infrared excess expected for Class II objects (Strom 1989, Skrutskie 1990). These variations were interpreted as indicative of a transition phase from Class II to Class III sources, during which the disc material begins to dissipate, revealing central cavities and annular gaps. To explain these features, astronomers were prompted to propose the presence of tidal interactions between the disc and embedded companions, providing remarkable potential hints of ongoing planet formation for the first time (Marsh & Mahoney 1992, 1993). For further insight into the observational aspects of transitional discs, refer to the reviews by Espaillat et al. (2014) and van der Marel (2023).

Over the next two decades, the field witnessed another notable leap as technological progress facilitated the deployment of highly sensitive observatories into space, aiming to mitigate atmospheric effects on optical and infrared radiation. During the 1990s, the Hubble Space Telescope (HST) acquired direct optical images of circumstellar discs around many more T Tauri stars (see e.g. O’Dell & Wen 1994; Burrows et al. 1996). Moving into the 2000s, observations from the Spitzer Space Telescope along with radiative transfer modelling efforts made substantial contributions to our understanding of the evolution of circumstellar matter by identifying additional discs with cavities and gaps in their dust distributions (D’Alessio et al. 2005; Calvet et al. 2005; Espaillat et al. 2007; Brown et al. 2007), further underscoring the dynamic nature of these environments and reinforcing our perspective on the crucial role they play in the formation of planetary systems.

The breakthroughs continued with the rise of advanced infrared-, millimeter-, and centimeter-wave interferometers, which enabled the direct and resolved observation of the emission structure of planet-forming discs. The Very Large Telescope Interferometer (VLTI), the Submillimeter Array (SMA), the enhanced Karl G. Jansky Very Large Array (JVLA), and the more recent Atacama Large Millimeter/submillimeter Array (ALMA) ushered in an era of high-angular and spectral resolution imaging of protoplanetary discs. Over the past decade, ALMA has taken the forefront of research in planet formation at (sub-)millimeter wavelengths due to its unparalleled sensitivity and resolution power.

### 1.1.3.2 The ALMA era

At the time of this thesis’s writing, ALMA holds the distinction of being the world’s largest and most sensitive instrument operating at millimeter and submillimeter wavelengths (ranging from 0.32 to 3.6 mm). Its primary array comprises 50 antennae, each with a diameter of 12 meters, strategically located at an altitude of 5000 meters in the Atacama desert of Northern Chile to minimise atmospheric contamination. This arrangement is further supplemented by a compact configuration that includes 4 x 12-meter and 12 x 7-meter antennae, designed to enhance ALMA’s ability to also study astronomical structures with large angular sizes with

heightened sensitivity. It has a dynamic interferometric design that enables array configurations spanning from approximately 150 meters to 16 kilometers, granting an exceptional angular resolution of up to 10 milliarcseconds in its most extended configuration. To put this into perspective, such a high angular resolution enables the distinction of Earth-to-Sun separations (1 au) at a distance of 100 pc (a typical distance to nearby star-forming regions), surpassing the Very Large Array by 10 times and outperforming the Hubble Space Telescope by a factor of 5 in this matter.

ALMA has transformed our approach to observing and comprehending protoplanetary discs, shedding light on the intricate physical and chemical processes that drive planet formation. It has revealed that protoplanetary discs can exhibit a high level of substructure in their dust distribution (see reviews by Andrews 2020; Bae et al. 2023), providing valuable insights that help constrain models regarding the presence and properties of planets (as in e.g. Dong et al. 2015; Bae et al. 2016; Zhang et al. 2018). Furthermore, it has enabled in-depth mapping of the gas physical structure of numerous discs through the analysis of molecular emission (as in e.g. Rosenfeld et al. 2013; Pinte et al. 2018a; Teague et al. 2018b; Dullemond et al. 2020). Indeed, ALMA is sensitive to a stunning variety of molecular lines emitted by these discs, granting us access not only to the radial and vertical distribution of chemical species but also to the thermodynamic properties and dynamics of the portion of the gas disc that they trace (see reviews by Miotello et al. 2023; Pinte et al. 2023). The core focus of this thesis lies in the study of the gas disc kinematics to identify planet-driven signatures through the analysis of molecular line data acquired with this instrument.

## 1.2 The hunt for planets in formation

In parallel with the advancements in protoplanetary disc observations, the quest for fully formed planets in extra-solar systems has also made significant strides over the past three decades driven by the development of novel detection methods and the capabilities of wide field space missions such as the Kepler mission and the ongoing Transiting Exoplanet Survey Satellite (TESS), alongside the emergence of highly precise ground-based spectrographs like the High Accuracy Radial velocity Planet Searcher (HARPS). Together, these instruments have identified a significant portion of the more than 5000 confirmed exoplanets to date<sup>1</sup>. The orbits of these objects have been estimated to span a range from as compact as one hundredth of Mercury’s orbital radius to as extended as  $\sim 6000$  au, and their masses found to vary from as low as 0.02 Earth masses to as high as 13.6 Jupiter masses<sup>2</sup>. Figure 1.3 illustrates the current distribution of exoplanet masses as a function of their orbital semi-major axes, highlighting the portion of the distribution that can be probed by ALMA through the observation of planet-induced signatures in discs.

<sup>1</sup>Visit [exoplanet.eu](http://exoplanet.eu) for up-to-date reports.

<sup>2</sup>Objects with masses exceeding  $13.6 M_{\text{Jup}}$  (or  $0.013 M_{\odot}$ ) have also been detected but they are categorised as brown dwarfs, which are substellar objects with sufficient mass to fuse deuterium in their cores but not massive enough to sustain hydrogen fusion as a star (Burrows et al. 1993).

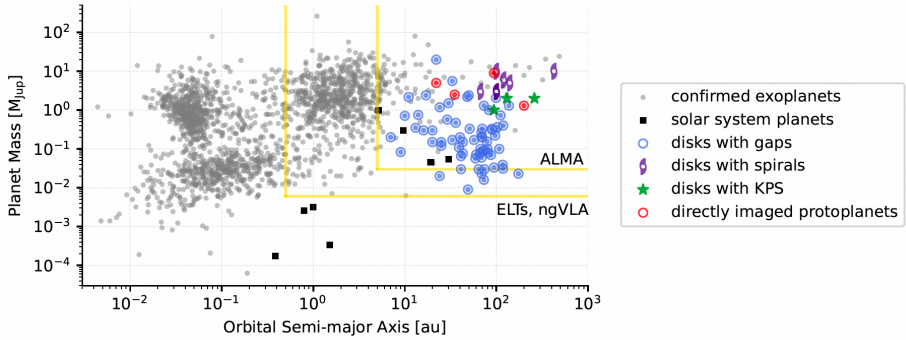


**Figure 1.3:** Illustrating the distribution of mass and orbital semi-major axis of confirmed exoplanets (grey circles), solar system planets (squares), directly imaged protoplanets (red circles) and protoplanets proposed based on observations of disc substructures (other symbols). Kinematic planet signatures (KPS, green stars) are associated with three Jupiter-mass planet candidates, one in the disc of HD 97048 proposed by Pinte et al. (2019), and two in the disc of HD 163296: one at a radial separation of  $R = 260$  au reported by the pioneering study of Pinte et al. (2018b) and confirmed in Chapter III, and another at  $R = 94$  au as identified in Chapter III using the methodology presented in Chapter II of this thesis. Credits: Bae et al. (2023).

Indeed, it is now firmly established that planets are remarkably diverse, not only in their gross physical attributes such as mass, size, and orbital parameters, but also in their chemical compositions. However, the exact formation pathways and conditions that lead to such variety of properties remain unknown. One way to reconstruct the history of this diversity is to go back in time by directly capturing the sites where planets are assembled in protoplanetary discs in order to make stringent comparisons with the properties of mature exoplanets. The challenge is that young planets are generally deeply embedded in their host disc, and therefore hard to observe due to the high extinction imposed by the surrounding material.

To date, PDS 70 is the only system in which (two) forming-planets have been convincingly detected through direct imaging of localised near infrared and  $H\alpha$  emission using VLT instrumentation (Keppler et al. 2018; Haffert et al. 2019), while other strong candidates await for confirmation in the discs of HD 169142 (Gratton et al. 2019) and AB Aur (Currie et al. 2022). The success of these detections can be attributed in large part to the fact that these objects are located in a region of the disc that has been substantially cleared of attenuating material. Infrared observations with the NACO adaptive optics instrument on the VLT have also facilitated the direct imaging of planets around relatively young stars such as Beta Pictoris (Lagrange et al. 2010), and HD 95086 (Rameau et al. 2013). Nevertheless, these systems have already transitioned to a debris disc stage in which most of the original gas and dust needed for planet formation have been dissipated or accreted, and the planets may have moved from their birth position. Another avenue for detecting young, still-embedded planets is through the use of indirect techniques, which involve studying the signatures that these bodies can

leave on their nascent environment. This is precisely where ALMA can act as a planet-hunting instrument.

High resolution continuum observations of discs with ALMA have revealed a striking amount of substructures in the dust distribution of numerous sources, ranging from rings and gaps, to arcs, filaments and spirals (see e.g. Andrews et al. 2018; Bae et al. 2023). Modellers have demonstrated that embedded planets are a reasonable explanation to the origin of many of these patterns (e.g. Dong et al. 2015; Bae et al. 2016; Zhang et al. 2018). However, this detection strategy is limited in that it requires strong assumptions on the dynamical properties of dust grains and local viscosity, which are still poorly constrained by observations, and also because planets are not the only possible driving mechanism capable to produce alike signatures in the dusty disc (see e.g. Andrews 2020). Figure 1.4 illustrates recent observations of dust substructures traced by millimeter and near infrared emission, and compares them to the dust signatures expected from planetary and non-planetary mechanisms.

As a workaround, the study of the disc kinematics at submillimeter wavelengths with ALMA has recently emerged as a promising alternative for detecting young, yet unseen planets in discs, through the analysis of velocity perturbations that these bodies trigger in the Keplerian rotation of the gaseous component. In the remainder of this chapter, I will outline the primary kinematic indicators of the presence of planets in discs and provide a summary of the pioneering observational discoveries that contributed to the emergence of this novel and rapidly expanding branch in the field of planet detection.

## 1.2.1 Planet signatures in gas discs: Theory

### 1.2.1.1 Analytical development

The theoretical exploration of the dynamical interaction between planets and discs rapidly garnered interest as soon as the notion emerged that planet formation should occur within flattened, gas-rich structures rotating around their parent stars. Although the theory of planet-induced perturbations to the physical and dynamical structure of discs can be traced back to the works of, for example, Goldreich & Tremaine (1980) and Papaloizou & Lin (1984), the mathematical foundation had already been well established in the study of the tidal interactions between the gravity of galaxies and their constituent stars, leading to the formation of galactic disc spirals (see Lindblad P.O. 1961; Lindblad B. 1962; Toomre 1969, and references therein). Governed by the same physical concept, a planet embedded in a disc, orbiting a star on a circular trajectory, exerts gravitational torques in the immediate vicinity of its Lindblad resonances which serve as the launching points for spiral density waves (Goldreich & Tremaine 1980), commonly referred to as *Lindblad* spirals. Figure 1.5 illustrates spiral perturbations induced by Jupiter-mass planets in the surface density and velocity field of a protoplanetary disc, as predicted by a numerical simulation.

Some of the outcomes of these early studies already indicated that fundamental properties of fully formed planets, such as their mass, orbital location, and

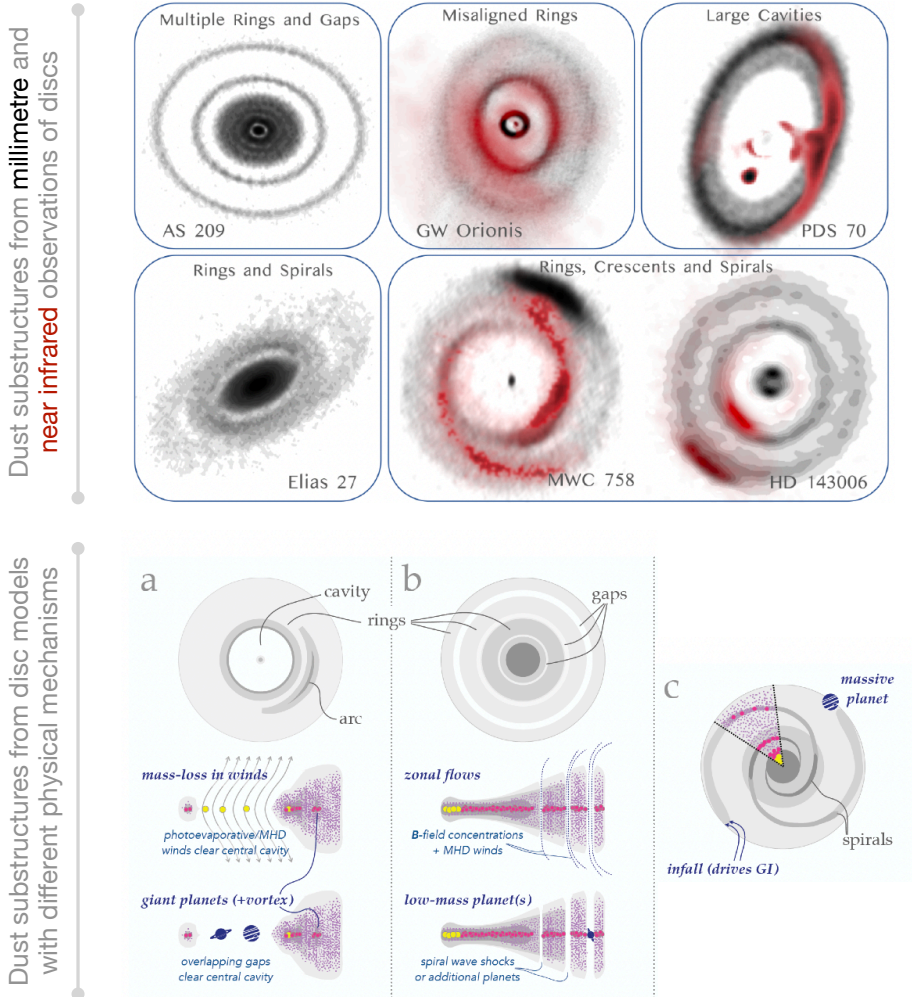


**Figure 1.4:** Dust substructures in protoplanetary discs, including gaps, rings, crescents and spirals. *Top panels:* Observed substructures in millimeter and near infrared continuum emission from real discs (adapted from Bae et al. 2023). *Bottom panels:* Plausible physical mechanisms explaining the presence of such substructures (adapted from Andrews 2020). While planets are one possibility, other processes could also account for the observed signatures.

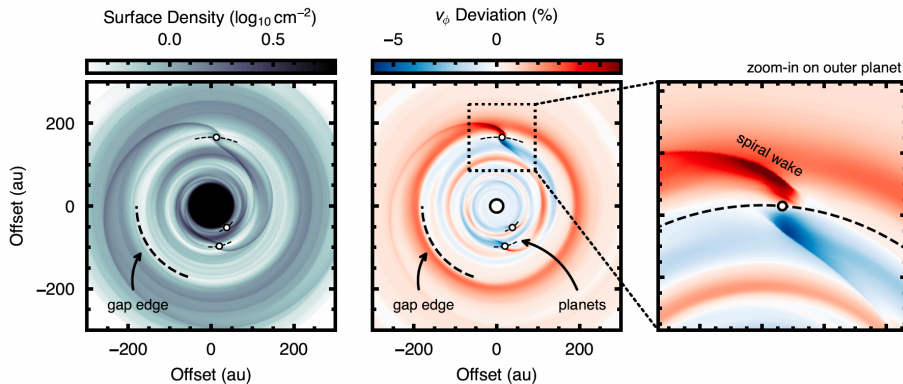


**Figure 1.5:** Snapshot from a planet-disc interaction simulation illustrating surface density (left) and percentage deviations from Keplerian motion (middle) triggered by the presence of Jupiter-mass planets. Spiral wakes and gaps are characteristic outcomes of the tidal interaction between discs and planets. Credits: Disk Dynamics Collaboration et al. (2020).

composition, could be significantly influenced by planet-disc dynamics. They concluded that the interplay between the planet-disc tidal interaction and dissipative forces inherent to the gas disc holds the potential to regulate the evolution of the disc (and thus accretion onto the protostar) through a net exchange of angular momentum from the inner to the outer parts of the system. Rafikov (2002a) enhanced the theory by incorporating observational features that were already known from planet-forming discs in the early 2000s, such as radially decreasing density and temperature distributions, as well as more realistic velocity shears. The author proposed analytical forms for mass accretion rates onto the star driven by the influence of planets, and demonstrated the importance of shock formation on the exchange of angular momentum through non-linear evolution of planet spiral waves, finding that even torques induced by low-mass planets ( $<10 M_{\oplus}$ ) could be significant drivers of both disc evolution and planetary migration.

### 1.2.1.2 Semi-analytic theory and the need for numerical models

With ALMA now enabling the resolution of subtle velocity fluctuations (on the order of a few  $10 \text{ m s}^{-1}$ ), recent studies have gained motivation to further develop the subtopic of spiral theory dealing with the structure and strength of the velocity perturbations carried by planet-driven waves. Recently, Bollati et al. (2021) showed that a semi-analytical form of this theory could offer qualitative predictions about the shape and magnitude of candidate planet perturbations observed in molecular intensity maps with ALMA (see Section 1.2.2). They found that the amplitude of the planet-induced velocity spiral, with an associated perturbation in the line intensity profile, goes as the square root of the planet mass at radii far from the planet, and scales linearly as the planet is approached. However,

while pedagogically informative, the current state of this approach comes with limitations as it is only applicable to planets below the thermal mass<sup>3</sup> for at least two reasons. First, the fact that the linear and non-linear evolution of the spiral waves cannot be effectively distinguished in the high-mass regime, upon which the semi-analytical solutions depend, as the waves themselves are initiated in a non-linear manner. And second, the presence of gaps would require a refactoring of the semi-analytical solutions as the assumed smooth background density field would no longer hold true.

Nevertheless, having gaps is not always detrimental when it comes to planet detection; in fact, it can be quite the opposite. The planet-disc tidal interaction has been long recognised for its capability to create gaps in the surface density of the disc, with significant consequences for the evolution of the entire system. A density gap could, for example, reduce the total mass that would be accreted by the star as much material from the outer disc may no longer drift toward the inner regions of the system. It can also lead to substantial decreases in the strength of planetary torques, thereby slowing down the initially rapid inward migration of the forming planet (see e.g. Rafikov 2002b).

Dynamical models of the disc gas have revealed that the presence of such substructures, and more broadly, of pressure fluctuations in the disc, results in concentric disturbances in the azimuthal component of the velocity field (Kanagawa et al. 2015; Rab et al. 2020), and potentially also in radial and vertical velocities in the form of meridional flows of material (Tanigawa et al. 2012; Morbidelli et al. 2014; Fung & Chiang 2016). The former can be understood through Eq. 1.6, where a pressure gradient localised radially acts as an extra central force pointing toward the centre of the gap. This pressure force opposes the gravitational force of the star at radii interior to the planet’s orbit, which in turn induces sub-Keplerian rotation around the inner edge of the gap in order to maintain centrifugal balance, and parallel to the star’s gravity exterior to the planet’s orbit, resulting in super-Keplerian rotation at the outer edge of the gap (as in Fig. 1.5). Meridional flows, on the other hand, arise from the interplay between planetary torques dominating near the disc midplane and viscous torques trying to fill up the gap from high layers far from the planet. This mechanism is thought to have substantial implications for planet mass accretion but also for planetary chemistry, as molecular species that might have been originally crafted in the disc atmosphere through energetic reactions can travel down to the midplane and eventually contribute to the chemical composition of planet atmospheres.

Moreover, morphological properties of planet-carved gaps such as the radial position, depth, and width, as well as induced kinematic features such as the amplitude of the associated velocity modulations, are intrinsically related to the orbital radius and mass of the planet in question, and to the local thermodynamic properties of the host disc such as the turbulent viscosity and pressure scale-height determined by the midplane temperature (Kanagawa et al. 2015, 2017). To self-consistently account for the response and correlations between these variables, it is possible to generate grids of numerical simulations in order to establish semi-

---

<sup>3</sup>The mass required for a planet to exert a torque strong enough such that the disc gas around it is repelled, forming a gap. It is written as  $m_{th} = 2/3(H_p/r_p)^3 M_*$  (Goodman & Rafikov 2001).



empirical laws relating planet properties and gap observables, including those from kinematics. Gyeol Yun et al. (2019), for example, derived a simple connection between the amplitude of the azimuthal velocity modulation  $\delta v_\phi$ , associated with a gap carved by a planet mass  $m_p$ , at an orbital radius  $R_p$ , for a turbulent viscosity  $\alpha$ , and a pressure scale height  $H_p$ ,

$$\frac{\delta v_\phi}{v_K} = \frac{H_p}{R_p} \frac{0.007K^{1.38}}{1 + 0.06K^{1.03}}, \quad (1.7)$$

where  $K \equiv (m_p/M_\star)^2(H_p/R_p)^{-5}\alpha^{-1}$ , and  $v_K$  is the Keplerian velocity given by Eq. 1.4. A notable limitation here lies in the uncertainty stemming from the disc properties (especially  $H_p$ , on which the planet mass depends steeply), for which we currently lack robust observational constraints. Nonetheless, this underscores the necessity of computational power to comprehensively address the impact of interconnected mechanisms on the physical and dynamical structure of discs. Powered by numerical simulations, our current view about gap formation also predicts that planets may create not only one but multiple gaps as each spiral arm excited by a planet can lead to the opening of an individual gap as they steepen into shocks, particularly in discs with low viscosity ( $\alpha < 10^{-4}$ ) where dissipation mechanisms are weak (see e.g. Bae et al. 2017).

### 1.2.1.3 Numerical simulations and observational predictions

In the last two decades, the majority of theoretical development on the signatures triggered by planets has been driven by numerical simulations that solve the equations of motion and conservation laws iteratively, and allow considering additional physical ingredients or even complex geometrical configurations. For example, these advancements have enabled the calculation of more realistic temperature structures in planet-disc interaction simulations through the incorporation of thermal relaxation processes such as radiation diffusion and gas-dust collision rates. This led to the discovery that planetary spirals are not limited solely to those induced by planetary torques at Lindblad resonances; if the thermodynamic conditions of the disc permit, spirals can also be launched from buoyancy resonances. These *buoyancy* spirals develop when the vertical temperature gradient of the gas disc is positive and its adiabatic index is larger than one, so long as the buoyancy frequency of the fluid at the planet location matches with the planet orbital frequency (Zhu et al. 2012; Lubow & Zhu 2014). As demonstrated by Bae et al. (2021), buoyancy spirals are more prone to develop in the outer disc at relatively high elevations over the midplane where the thermal relaxation is slow due to infrequent gas–dust collisions.

The magnitude of the velocity perturbation carried by buoyancy spirals is expected to increase with height over the disc midplane due to the usually more pronounced temperature gradients as the disc atmosphere is approached. Furthermore, the vertical velocity component dominates along the spine of these spirals, and their pitch angles are expected to always be low ( $< 10$  deg), making these structures render as tightly wound, almost circular signatures in the disc velocity field. Lindblad spirals, on the other hand, differ morphologically as they display

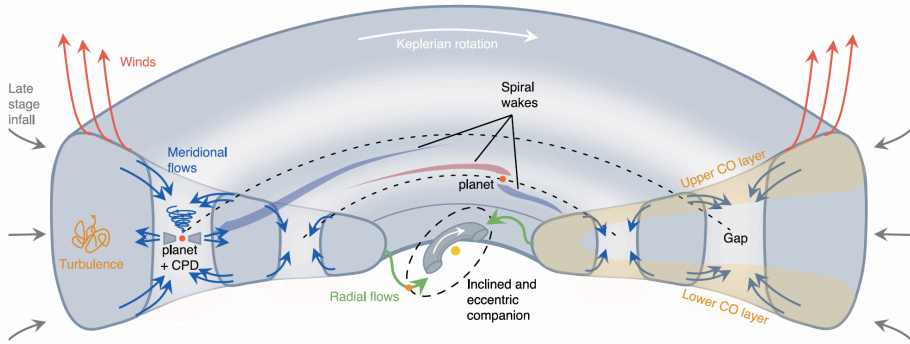


**Figure 1.6:** Schematic overview of some of the signatures expected from planet-disc interaction in gas discs. Also shown are other processes linked to the disc evolution such as late stage infall from the remnant envelope and winds. Credits: Pinte et al. (2023).

decreasing pitch angles as one moves away from the planet. Also, as opposed to buoyancy spirals, the velocity structure of Lindblad spirals is primarily dominated by radial and azimuthal motions, with magnitudes that diminish vertically as one moves away from the disc midplane (see Rabago & Zhu 2021; Bae et al. 2021).

Several modelling efforts have also enabled the understanding of how these density and velocity perturbations caused by a planet would appear in real observations. Using planet-disc interaction simulations and simultaneously calculating the radiation transport for the distribution of density, temperature, and velocities of the perturbed disc, Pérez et al. (2015, 2018) found that deviations from Keplerian motion should result in observable localised and large-scale fluctuations in molecular line emission obtained with ALMA. Not long after, the first observational confirmation of similar features would come to light in the disc of HD 163296 (see Section 1.2.2). Following a similar methodology, Dong et al. (2019) demonstrated that the interplay between planetary and viscous torques can produce increased velocity dispersions in the gas disc, which could in turn be observed as broadened molecular line profiles.

Figure 1.6 provides a schematic overview summarising some of the planet-disc interaction signatures discussed in this section, as predicted by theoretical models. These signatures include (1) axisymmetric substructures such as gaps, resulting in azimuthal and meridional velocity flows, as well as increased velocity dispersions near the gapped region, (2) non-axisymmetric features such as spiral waves, with varying opening angles and magnitudes that depend on the driving mechanism and on the height where they are measured with respect to the disc midplane, and (3) localised high-amplitude velocity perturbations in the immediate vicinity of the planet. The purpose of the following section is to outline the observational signatures that have been reported in recent studies as being potentially related to the interaction between discs and planets.

### 1.2.2 Planet signatures in gas discs: ALMA Observations

ALMA, unlike any other instrument, has granted us access to the bulk gaseous component of protoplanetary discs, enabling us to explore numerous aspects that may significantly influence the formation and composition of planets. For example, it provides the means to investigate the three-dimensional structure of discs by simultaneously observing multiple molecular tracers and lines (see Miotello et al. 2023, for a review). Through the analysis of the morphology and velocity shifts of these lines, we can also investigate internal fluctuations in the disc temperature and kinematics, while also inferring interconnected attributes such as gas density and pressure (see e.g. Teague et al. 2018a; Dullemond et al. 2020; Yu et al. 2021). Molecular line studies with ALMA further enable us to quantify non-thermal motions (see e.g. Flaherty et al. 2020, and references therein), estimate stellar (as in Czekala et al. 2017) and disc masses (Veronesi et al. 2021; Lodato et al. 2022), and, pertinent to this thesis, identify signatures from planet-disc interaction.

From theory (Sect. 1.2.1), we have learned that typical amplitudes for planet-driven velocity perturbations are on the order of  $0.1 \text{ km s}^{-1}$ . This makes observations dedicated to studying such fine motions require spectral channels of a similar spacing if we are to distinguish planet-induced velocities from the rotation pattern of the disc. However, narrowing the channel spacing requires an increase of the same factor in the integration time of the observation to keep the same signal-to-noise ratio (since  $S/N \propto \sqrt{t_{\text{obs}} \Delta v}$ ) and effectively improve the velocity precision. Consequently, observational surveys designed to systematically characterise protoplanetary discs at high resolutions require substantial execution times to achieve their goals in a robust manner. For example, the large program Molecules with ALMA at Planet-forming Scales (MAPS, Öberg et al. 2021) demanded around 130 hours of telescope time to study the chemical structure of five discs across more than 40 different spectral lines at a notable velocity resolution of  $0.2 \text{ km s}^{-1}$ .

For a similar reasoning, the majority of the kinematical studies focused on the detection of planet-driven signatures in discs have been carried out using abundant and bright molecular tracers such as CO and its main isotopologues,  $^{12}\text{CO}$ ,  $^{13}\text{CO}$ , and  $\text{C}^{18}\text{O}$ , in rotational transitions with low excitation energies (usually  $J = 2 - 1$  and  $J = 3 - 2$ ) which ensure that the molecule is excited at temperatures sufficiently low, typical of protoplanetary discs ( $T < 100 \text{ K}$ ) in their outer regions ( $R > 10 \text{ au}$ ) resolvable by ALMA without further compromising sensitivity<sup>4</sup>. An ongoing planet-hunting campaign, the exoALMA large program<sup>5</sup>, focuses mainly on  $^{12}\text{CO}$  and  $^{13}\text{CO}$   $J = 3 - 2$  lines (and still required 180 hours of telescope time) to fully exploit ALMA’s capabilities to search for planets in 15 discs at an exceptional velocity resolution of  $0.028 \text{ km s}^{-1}$ .

Another key aspect that enhances the precision and accuracy of current kine-

---

<sup>4</sup>Even though  $\text{H}_2$  is the main constituent of the bulk disc gas, it is not well suited for dynamical studies of such cold and quiet environments because even its lowest ro-vibrational levels require high amounts of energy to be excited (Wolfire & Konigl 1991; Habart et al. 2005), and although its lowest pure rotational transition can be excited at  $\sim 100 \text{ K}$ , it is weak and unresolved in velocity (Thi et al. 2001). CO, on the other hand, is easily excited by collisions and is the second most abundant molecule, with typical CO/ $\text{H}_2$  ratios between  $10^{-5}$ – $10^{-4}$  (Miotello et al. 2014)

<sup>5</sup><https://www.exoalma.com/>

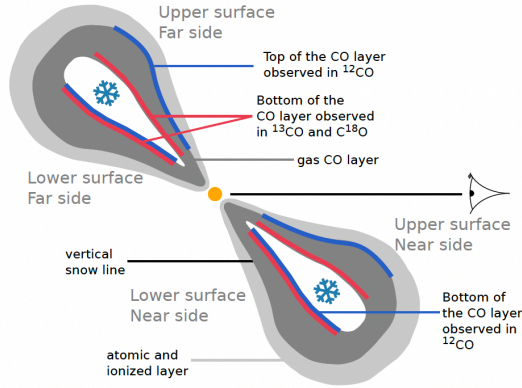


**Figure 1.7:** Schematic edge-on view of the vertical structure of the gas component of a protoplanetary disc highlighting the overall CO distribution in its gas phase.  $^{12}\text{CO}$  line emission seen by an observer (on the right hand side of the sketch) would primarily probe the disc upper layers due to its high optical depth. The bottom of the CO layer, closely related to the vertical snowline of the tracer, can also be observed along specific sight lines favoured by projection and reduced optical depth of the top layer emission towards the wings of the line profile (see Fig. 1.8). Optically thinner isotopologues such as  $^{13}\text{CO}$  and  $\text{C}^{18}\text{O}$  are expected to probe intermediate layers. Credits: Pinte et al. (2018a).

mathematical studies of discs is the ability of ALMA to resolve the vertical structure of these objects through the simultaneous observation of multiple molecular tracers. For example, as  $^{12}\text{CO}$  tends to be dense, optically thick, and distributed across a substantial portion of the disc, its emission often originates from elevated layers ( $z/r \approx 0.3$ ) above the midplane, as depicted in Figure 1.7. Conversely, optically thinner isotopologues like  $^{13}\text{CO}$  and  $\text{C}^{18}\text{O}$  are more likely to emit from lower altitudes ( $z/r \approx 0.1 - 0.2$ , see e.g. Law et al. 2021b; Paneque-Carreño et al. 2023). In cases where the disc surface density is high enough to a point where effective heating from stellar irradiation is hindered, temperatures at the midplane can plummet to values below 20 K. At these low temperatures, CO freezes onto dust grains, establishing a chemical barrier that restricts how deeply our line observations can penetrate along the disc vertical direction. Nevertheless, this vertical snowline can also be observed through analysis of emission from the backside of sufficiently inclined sources (Dullemond et al. 2020), which grants invaluable insight into the temperature structure of discs in regions near the midplane, where the majority of planet formation processes actually unfold.

Figure 1.8 illustrates the projected pattern of the  $^{12}\text{CO}$   $J = 2 - 1$  line emission for the disc around HD 163296, observed with ALMA at an angular resolution of  $0.1''$  and a channel spacing of  $0.32 \text{ km s}^{-1}$  (Andrews et al. 2018; Isella et al. 2018). The morphology of the intensity channels is the result of a combined effect between the quasi-Keplerian rotation of the disc and projection given by the disc inclination and vertical structure. From Section 1.1.2, we know that Keplerian motion

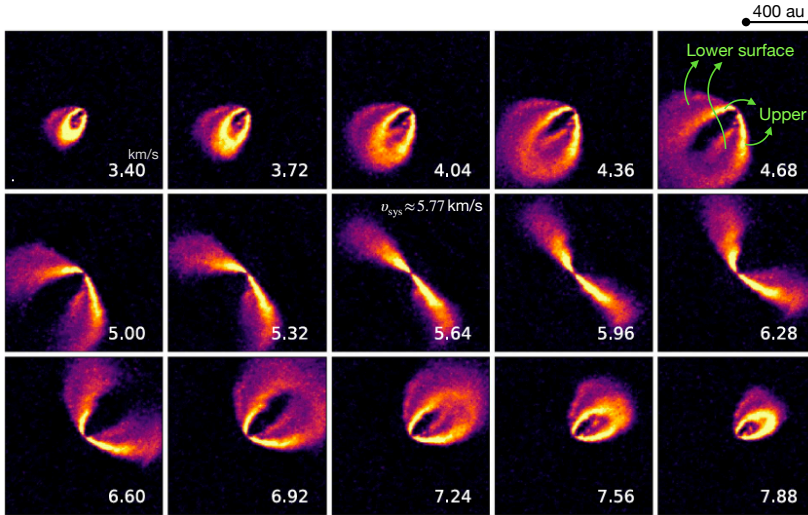


**Figure 1.8:**  $^{12}\text{CO } J = 3 - 2$  line intensity channels for the disc around HD 163296 as observed with ALMA, adapted from Isella et al. (2018). The size of the synthesized beam is  $0.''104 \times 0.''095$ , which corresponds to a physical resolution of around 10 au at the distance of the source (101.5 pc). Velocity channels are spaced every  $0.32 \text{ km s}^{-1}$ . For reference, the systemic velocity of the source is  $5.77 \text{ km s}^{-1}$  according to model channel maps presented in Chapter III for the same target.

is characterised by increasingly high velocities near the central star and decreasing values with orbital radius as  $v_\phi \propto R^{-1/2}$ . This causes the innermost orbits to dominate the emission pattern of higher velocity channels. Intermediate velocity channels on the redshifted and blueshifted sides of the disc adopt a teacup-like form, relatively symmetric except for the projection effect imposed by the vertical structure of the disc. This particular shape emerges because a given velocity value, projected along a specific sight line, is achieved twice within a single orbit – once on the near side and once on the far side of the disc with respect to the observer – as long as the velocity of the intensity channel analysed is smaller than the maximum velocity that can be projected along the orbit. Finally, as the velocity of the examined channel nears the systemic velocity of the source, the intensity pattern stretches, as it now traces regions of the disc tangential to the line of sight.

Now, if the disc rotational motion is perturbed by a planet, the projected velocity of a gas parcel near the planet will deviate from the purely quasi-Keplerian behavior. Consequently, emission from this gas parcel should manifest in adjacent velocity channels, resulting in an observable wiggle, or *kink*, in the projected intensity of the molecular line. This phenomenon was reported for the first time by Pinte et al. (2018b) using  $^{12}\text{CO}$  ALMA observations of the disc of HD 163296, as displayed in Figure 1.9, marking the beginning of a novel method for detecting young planets in their early stages. In their study, the authors produced a grid of synthetic observations from planet-disc interaction simulations with vary-

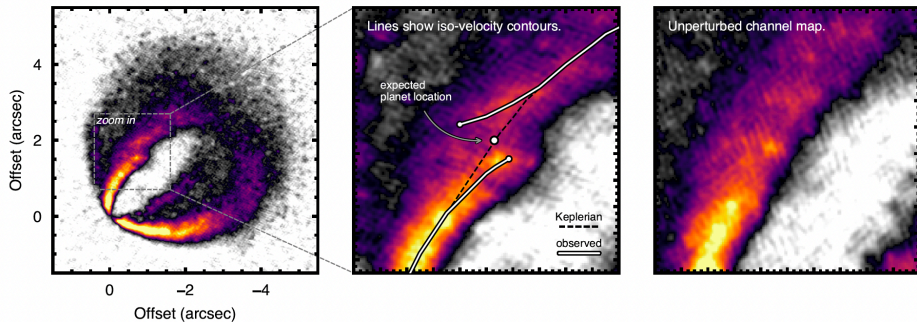


**Figure 1.9:** First intensity kink reported in a protoplanetary disc, the disc of HD 163296, as being associated with an embedded planet (Pinte et al. 2018b). The kink was observed with ALMA, in  $^{12}\text{CO}$  emission, and is the result of high-amplitude deviations from Keplerian rotation attributed to a  $2 M_{\text{JUP}}$  planet at a radial separation of 260 au from the central star. Also shown is an unperturbed channel observed on the other side of the disc (and flipped for better comparison) to illustrate the intensity pattern expected from smooth rotation. Credits: Disk Dynamics Collaboration et al. (2020).

ing planet masses aiming at replicating the apparent amplitude of the observed intensity kink. The results revealed that a planet with a mass of  $2 M_{\text{JUP}}$ , situated at an orbital radius of 260 au, yielded a reasonable match between the amplitude and morphology of the synthetic and observed kinks.

In parallel, Teague et al. (2018a) studied the same source and reported radially localised modulations in the rotation curves traced by CO isotopologue emission due to the presence of gaps, though at smaller orbital separations compared to the kink-like feature. The authors invoked giant planets of the order of Jupiter’s mass to explain the amplitude of these perturbations, with the caveat that this method alone is unable to tell whether the gaps in question are planetary in origin. Not long after, high-resolution  $^{13}\text{CO}$  observations allowed the detection of a new kink, this time in the disc around HD 97048 (Pinte et al. 2019), again associated with the presence of a giant planet at an orbital radius of 130 au, co-spatial with a dust gap observed in millimeter continuum. Pinte et al. (2020) would carry out a larger study of the presence of kinks in 18 additional systems, finding that at least eight of these discs exhibit tentative signatures in intensity channels that could be related to localised perturbations driven by embedded planets.

### 1.3 This thesis

As the field’s attention turns towards acquiring deep, high angular and velocity resolution data to gain insights into the presence of embedded planets, the apparent disturbances in molecular line emission will become more frequent and noticeable. Naturally, the question arises: how reliable are these detections, and, more importantly, which of them can be confidently classified as outcomes from planet-disc interaction? This thesis centres on identifying and quantifying kinematic signa-

tures driven by planets in discs in a statistically meaningful manner, presenting a methodology grounded in the detection of perturbations in line profile observables through simple parametric models of the disc dynamical structure. The following sections outline the chapters and conclusions of this dissertation,

**Chapter II. A robust technique to detect young planets in discs.** Localised velocity perturbations serve as powerful indicators of the presence of planets in discs. This chapter introduces a modelling and analysis framework, named DISCMINER, designed to replicate the channel-by-channel intensity of molecular lines originating from protoplanetary discs assuming smooth and Keplerian parametric profiles to represent the observed emission. Utilising this framework, we extract observable velocity perturbations from a range of planet-disc interaction simulations, incorporating different planet masses and azimuthal positions. Subsequently, a clustering technique is employed to identify coherent fluctuations within the disc’s velocity field, and measure their amplitude and variance. This approach demonstrates the potential to precisely infer not only the radial but also the azimuthal position of an embedded planet through the detection of perturbations that are significantly strong and localised in relation to the disc’s rotation pattern. Another significant finding presented in this chapter is that the variance of peak velocity perturbations is amplified in the vicinity of the planets, which could serve as a quantitative criterion for planet detection in future surveys.

**Chapter III. A new planet candidate in the disc of HD 163296.** The disc of HD 163296 offers an ideal backdrop for the search for signatures of planet-disc interactions as it was the first source associated with observed kinematic signatures from planets. In this chapter, we apply the DISCMINER modelling and statistical framework to ALMA observations of the  $^{12}\text{CO } J = 2 - 1$  line emission from the HD 163296 disc, taken at high angular resolution. Our analysis indicates that the prominent kink-like feature initially identified in intensity channels, at a radial distance of 260 au, is attributed to both a localised velocity perturbation and an extended spiral structure that might indeed be driven by a massive embedded planet as originally proposed by Pinte et al. (2018b). Moreover, in this chapter we present the detection of strongly localised velocity perturbations, possibly related to the presence of a Jupiter-mass planet, situated at a radial distance of 94 au and azimuth of  $50^\circ$ , near the centre of a dust gap observed in millimeter continuum.

**Chapter IV. Extended search for planet-disc interaction signatures in multiple sources and CO isotopologues.** Localised perturbations are not the sole observable signature produced by planets in discs; large-scale perturbations and line broadening are also crucial features. This chapter embarks on a quest for new planet candidates and applies the same methodology presented in previous chapters to a broader range of protoplanetary discs and molecular tracers. The sample under analysis includes the discs around HD 163296, MWC 480, AS 209, IM Lup, and GM Aur, observed in  $^{12}\text{CO}$ ,  $^{13}\text{CO}$ , and  $\text{C}^{18}\text{O}$  line emission as part of the ALMA large program MAPS (Öberg et al. 2021). This chapter reveals that all these sources exhibit a striking degree of substructure, encompassing not only velocity but also line width and intensity variations. Localised velocity perturbations are confirmed in the HD 163296 disc in  $^{12}\text{CO}$  and, for the first time, in  $^{13}\text{CO}$  as well. Additionally, line width increments are consistently detected across

all CO isotopologues near the new planet candidate reported in Chapter II for this disc. Large-scale meridional flows are unveiled in the discs of MWC 480 and AS 209. In the case of MWC 480, the vertical modulation of these flows and their tightly wound morphology suggest a potential connection to planet-induced buoyancy spirals. Prominent line width enhancements on one side of the disc, at the same radial separation as the candidate spirals, offer insights into the azimuthal location of the embedded planet. In the disc of AS 209, the vertical motions align with upward velocities, marking the presence of winds. Notably, significant line broadening is also observed in this source, at the radial and azimuthal location of a circumplanetary disc candidate proposed by Bae et al. (2022). This chapter also underscores that the simultaneous utilisation of line width and velocity profiles constitutes a potent approach for identifying pressure fluctuations in discs.

**Chapter V. Enhanced methodology for planet detection in exoALMA targets.** The exoALMA large program will provide unprecedented insights into the structure of 15 circumstellar discs where planet formation might be ongoing. This chapter introduces an improved methodology, built upon the DISCMINER framework, aimed at detecting gas substructures and potential planet-induced signatures within the exoALMA target discs. These targets are observed in  $^{12}\text{CO}$ ,  $^{13}\text{CO}$ , and CS lines at high angular resolutions ( $0.1'' - 0.15''$ ) and unmatched velocity resolutions ( $28 - 100 \text{ m s}^{-1}$ ). The methodology is illustrated using the discs of HD 135344B, LkCa 15, and MWC 758 as examples. In the case of HD 135344B, robust evidence emerges for the presence of unseen companions. Through analysis of velocity and line width perturbations, we propose three planet locations: a massive planet at 76 au with significant velocity dispersions across multiple vertical layers, a closer-in planet at 42 au causing enhanced velocity dispersions in upper layers, and an outer planet at 100 au leading to a Doppler flip associated with a spiral perturbation in the gas. These companions are believed to be connected to observed dust continuum substructures including cavities, crescents, and a two-armed spiral. In the disc of MWC 758, the presence of multiple massive embedded planets is suggested in order to explain both large-scale kinematic signatures and near-infrared spirals: an inner giant planet at 30 – 40 au, and an outer planet at 100 au triggering a tightly wound velocity spiral. Three-dimensional hydrodynamical simulations of planet-disc interaction are also presented in this chapter to demonstrate the close relationship between the location of planets and localised line width perturbations. This study lays the groundwork for upcoming endeavours centred on the exploration of protoplanetary discs and the detection of young planets using molecular line tomography.

The key contributions and conclusions of this thesis are as follows,

- A statistical methodology that harnesses coherent velocity and line width perturbations to robustly identify embedded planets is introduced for the first time. This approach not only reveals the orbital radius but also pinpoints the azimuthal location of the perturbing planet with high precision.
- Coherent localised velocity perturbations are powerful indicators of the presence of planets. Although most of these features manifest as kinks in intensity



channels, not all kinks are unequivocally associated with localised kinematic signatures and planets.

- A comprehensive approach that encompasses the study of not only velocity variations but also perturbations in the morphological properties of line profiles observed across multiple molecular tracers is paramount for a robust identification and characterisation of planet-induced signatures.
- Precise mapping of line profiles also enables a three-dimensional tomography of the physical and dynamical structure of discs. Some applications include studying the disc's radial and vertical temperature distribution, identifying gas gaps and over-densities, and estimating dynamical masses and disc geometry through channel-map modelling.
- Among the eight discs analysed in this thesis, five exhibit signatures potentially linked to massive planets forming at wide orbits ( $R > 50$  au). If future surveys confirm that this trend is widespread in large discs, gravitational instabilities are likely to play a dominant role in shaping the dynamical evolution of these objects and the formation of planets at early stages.

## 1.4 Future prospects

An unambiguous characterisation of molecular line features driven by planetary versus non-planetary mechanisms is missing in the field. Although we possess a solid theoretical and observational foundation regarding the signatures resulting from planet-disc interaction, evidence suggests that planets do not form in isolation. More likely, they coexist with other physical mechanisms operating in discs, such as gravitational instabilities (GI), vertical-shear instabilities (VSI), magneto-rotational instabilities (MRI), and even the influence of internal and external stellar companions. Independent modelling endeavours have revealed that the interplay between discs and these non-planetary processes gives rise to a spectrum of distinct patterns as well. However, a comprehensive characterisation of the specific features discernible through molecular line emission, which is what we can observe with instruments like ALMA, is still lacking, particularly in the context of composite scenarios including the presence of planets.

Certainly, such a characterisation poses a significant computational challenge as it needs to account for a wide range of ingredients, including the disc's physical properties that lead to the aforementioned instabilities and their various regimes, the properties of the planets which may influence how these processes develop and evolve, and the observational parameters that dictate whether these features can be distinguished and successfully classified. Nevertheless, the advancement of new numerical methods based on artificial intelligence algorithms, which are only just beginning to be explored in the field of planet formation, may prove to be an invaluable aid and propel these types of studies like never before.

On the observational side, ongoing and forthcoming technological advancements will significantly drive the field in the next decade. In parallel with surveys

dedicated to the direct imaging of planets using current cutting-edge instruments like JWST and MagAO-X, the exceptional resolution and sensitivity capabilities of the upcoming Extremely Large Telescope (ELT) will play a crucial role in deepening our understanding of planet formation processes taking place within the innermost few astronomical units of discs, where Earth-like and most giant planets are expected to assemble. More specifically, the Mid-infrared ELT Imager and Spectrograph (METIS) will be highly complementary to the spatial and temperature regimes accessible to ALMA in protoplanetary discs. This instrument will be capable of observing the warm inner regions of discs at spatial resolutions  $\sim 5 - 10$  times higher than those attainable by ALMA, offering unique insights into the distribution of small dust particles shaped by nascent planets at Solar System scales. METIS may also hold the potential to identify thermal continuum emission from young warm Neptune-like planets, and allow us not only to detect hot accretion signatures emanating from circumplanetary discs around Jovian planets but also to resolve the dynamical structure of these flows, providing a direct view into the process of planet assembly for the first time. This instrument will also offer exceptional access to the inner gas disc kinematics, especially through high-resolution observation of the ro-vibrational CO lines at 4.7 microns, which could be actively exploited in the context of young planet detection using the methodologies presented and demonstrated in this thesis.

